

Weakly correlated one-dimensional indium chains on Si(111)

Jun-Hyung Cho,¹ Dong-Hwa Oh,¹ Kwang S. Kim,² and Leonard Kleinman¹¹Department of Physics, University of Texas, Austin, Texas 78712-1081²Center for Superfunctional Materials, Pohang University of Science and Technology, Pohang 790-784, Korea

(Received 11 June 2001; published 14 November 2001)

Quasi-one-dimensional (1D) metals often exhibit a broken symmetry state. Here our first-principles density-functional theory calculations show that quasi-1D indium chains on the Si(111)-(4×1) surface are stabilized with (4×2) or (8×2) symmetry by lattice distortions of the two zigzag indium rows composing the chain. The ground state is almost degenerate, consistent with recent experiments which indicate that several phases coexist at low temperature.

DOI: 10.1103/PhysRevB.64.235302

PACS number(s): 68.35.Bs, 68.35.Rh, 73.20.-r

It is very challenging to understand the nature of phase transitions recently observed in one-dimensional (1D) metallic chains on silicon substrates.¹⁻³ These quasi-1D materials have been a fascinating subject to material scientists, because of the technological importance of the formation of atomic-scale structures. Due to recent developments in lithography, the size of electronic devices can be reduced to the atomic limit where quasi-1D materials are anticipated for atomic-scale interconnects.

Indium atoms are known to form quasi-1D chains on a (4×1)-reconstructed Si(111) surface.⁴⁻⁷ The correct structural model of this (4×1) surface reconstruction has been a longstanding issue. Unlike several qualitative structural models proposed earlier,^{4,6} a recent x-ray-diffraction experiment⁷ determined a detailed structural model for the indium-induced Si(111)-(4×1) surface, which is consistent with previously existing experimental data. It was recently reported that this system undergoes a reversible phase transition from a room-temperature (4×1) structure to a (4×‘2’) structure at about 100 K, driven by a 1D charge-density wave (CDW) or, equivalently, a Peierls instability along the indium chain.² Here ‘2’ indicates the presence of half-order streaks rather than peaks in a reflection high-energy electron-diffraction pattern. Subsequently an x-ray-diffraction experiment³ observed a well-developed (8×) superstructure in the direction perpendicular to the indium chains, but half-order streaks along the chains still persist even at 20 K. This result apparently indicates that this system does not exhibit a simple quasi-1D CDW-driven transition, because at 20 K the CDW has not yet condensed into a superstructure even though a good transverse chain-to-chain coupling was established. Based on the analyzed atomic structure of the low-temperature (8×‘2’) phase from x-ray-diffraction data,³ the new driving force for the phase transition was a proposed reduction in the total free energy due to trimer formation of the indium atoms. Thus the driving force behind the phase transition is still controversial, while a detailed atomic structure of the low-temperature phase remains uncertain.

In this paper we investigate the surface reconstruction and the electronic structure of the In/Si(111) system, based on first-principles density-functional theory calculations. Our results for the (4×1) structure give a successful theoretical reproduction of the measured angle-resolved photoemission

(ARP) band structure,⁸ scanning tunneling microscopy (STM) images,^{5,6} and core-level photoemission data.⁹ The calculated atomic structures for the (4×2) and (8×2) reconstructions agree in many but not all respects with the interpretation of the x-ray-diffraction data in Ref. 3.

Our first-principles calculations were performed using norm-conserving pseudopotentials¹⁰ and the generalized gradient approximation (GGA).¹¹ The Si(111) substrate is simulated by a repeating slab model of six Si atomic layers (not including the Si surface chain). The bottom of the slab has a bulklike structure, with each Si atom saturated by one H atom. A 10.4-Å vacuum region between H and outer In atomic planes is included. The electronic wave functions are expanded in a plane-wave basis set with a cutoff energy of 15 Ry. The **k**-space integrations in various unit-cell calculations are done equivalently with 64 **k** points in the surface Brillouin zone (SBZ) of the (4×1) unit cell. The position of all atoms, except the innermost Si layer atoms, held at their calculated bulk positions ($a_0 = 5.47$ Å), are allowed to relax along the calculated Hellmann-Feynman forces until all the residual force components are less than 1 mRy/bohr.

First we present our results for the atomic and electronic structures of In/Si(111)-(4×1). The optimized atomic structure within a recently proposed structural model⁷ is shown in Figs. 1(a) and 1(b). A quasi-1D indium chain is composed of the two zigzag rows *A* and *B* [see Fig. 1(b)], each of which contains two indium atoms per unit cell. Note that in each row the indium atoms are located at different adsorption sites. The height differences of the indium atoms are $\Delta h_{\text{In}_1-\text{In}_3} = 0.46$ Å and $\Delta h_{\text{In}_2-\text{In}_4} = 0.50$ Å, and the distance between top-layer atoms are $d_{\text{In}_1-\text{In}_3} = 3.04$ Å, $d_{\text{In}_2-\text{In}_4} = 3.03$ Å, $d_{\text{In}_3-\text{In}_4} = 3.12$ Å, and $d_{\text{In}_1-\text{Si}_2} = d_{\text{In}_2-\text{Si}_1} = 2.67$ Å. The bond lengths from In₃ and In₄ to the Si substrate are 2.71 and 2.72 Å, respectively. The overall structures of the indium chain and the silicon substrate agree well with x-ray-diffraction data.⁷ The calculated band structure for the (4×1) structure is shown in Fig. 2(a). We find four surface-state bands S_1 , S_2 , S_3 , and S_4 near the Fermi level. Remarkably, the dispersions of these surface-state bands along high-symmetry lines are in good agreement with ARP data.⁸ The charge character of these surface states, shown in Fig. 2(c), reveals that the S_1 and S_2 states represent appreciable indium-*p* character hybridized with neighboring Si

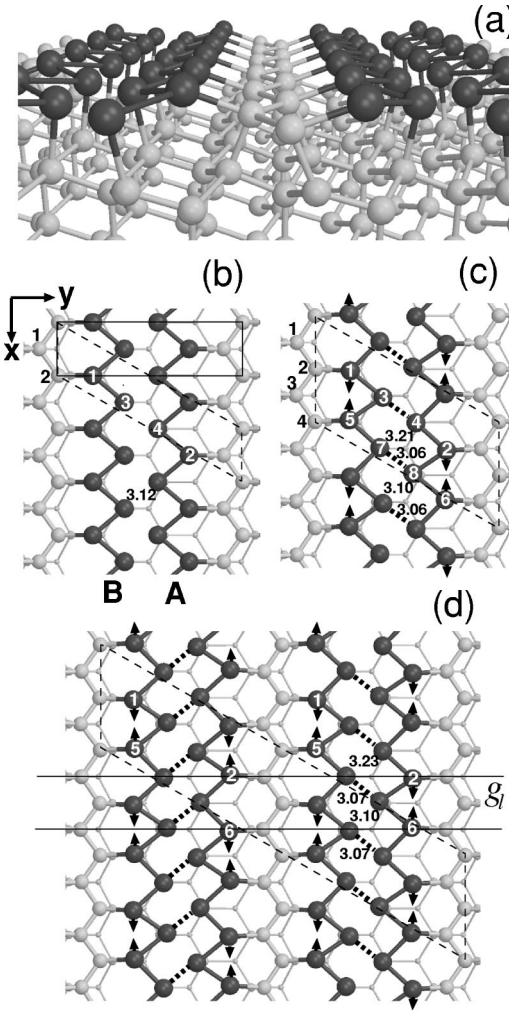


FIG. 1. Equilibrium structure of In/Si(111): (a) the perspective view of the (4×1) structure and the top views of (b) the (4×1) structure, (c) the (4×2) structure, and (d) the (8×2) structure. The dark and grey circles represent In and Si atoms, respectively. The x and y directions are $[\bar{1}10]$ and $[11\bar{2}]$, respectively. Two different choices for the (4×1) unit cell are indicated by the thin solid and dashed lines. The arrows in (c) and (d) show pairing patterns of the outer indium atoms. The solid lines g_l in (d) represent the equivalent glide lines. The interatomic distances between the two zigzag indium rows are given in Å.

states, whereas the S_3 (S_4) state mainly originates from Si substrate states, contributing to the interface bonding between the indium atom 3 (4) and the underlying Si substrate atom. Simulated STM images for the filled and empty states, shown in Figs. 3(a) and 3(b), are also in good agreement with the STM measurements.^{5,6} In the filled-state image [Fig. 3(a)] the brightest regions represent the p_z orbitals of the “inner” indium atoms 3 and 4. Here the asymmetric images for the two zigzag indium rows are due to different contributions of the four surface states which have site-dependent charge characters on each row [see Fig. 2(c)]. The empty-state image shows two line images related to the “outer” indium atoms 1 and 2.

Our band-structure calculations for In/Si(111)- (4×1) show that the S_3 state crosses the Fermi level at almost the

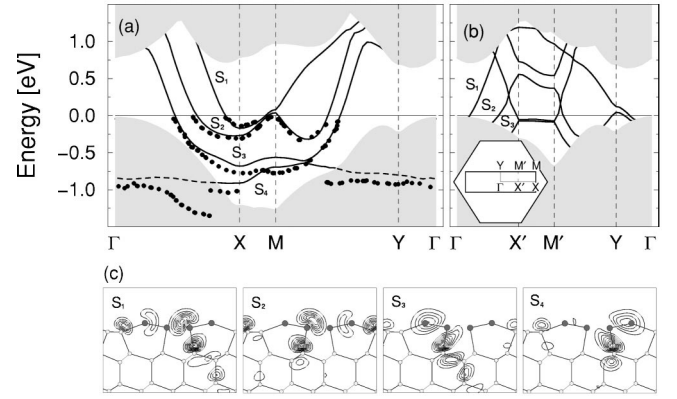


FIG. 2. Surface band structure of (a) In/Si(111)- (4×1) and (b) In/Si(111)- (4×2) . The inset in (b) shows the surface Brillouin zone for the (4×1) and (4×2) unit cells with that for the (1×1) unit cell as a reference. Shaded areas are the projected bulk-band structure. Filled circles represent the ARP data of Abukawa *et al.* (Ref. 8). (c) Charge characters of the surface states S_1 , S_2 , S_3 , and S_4 at the X point in the (4×1) structure. The plots for S_1 and S_4 (S_2 and S_3) are drawn in the vertical yz plane containing In_1 and In_4 (In_2 and In_3). The contour spacings are $0.0675e/\text{Å}^3$.

midpoint of the symmetry lines ΓX and YM (at $0.48 \overline{\Gamma X}$ and $0.48 \overline{YM}$). This crossing of the S_3 state is found to show no dispersion along the XM direction. It is expected that a charge density wave coupled to a lattice vibration of wavelength $2a_{[11\bar{1}0]}$ along the indium chains might lead to a Peierls-like instability.² To examine this possibility, we performed an optimization of the symmetry-unrestricted geometry within the (4×2) and (8×2) unit cells, employing the indium-trimer geometry (reported in Ref. 3) as the initial one. Our optimized (4×2) and (8×2) structures are shown in Figs. 1(c) and 1(d), respectively. We find that the (8×2) structure is more stable than the (4×2) structure by 0.9 meV per (4×1) unit cell, and that both structures are more stable than the (4×1) structure by about 8 meV per (4×1) unit cell. Our band structures for the (4×2) structure [Fig. 2(b)]

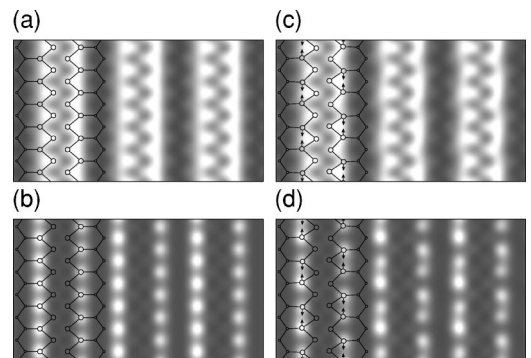


FIG. 3. Simulated STM images of In/Si(111)- (4×1) and In/Si(111)- (4×2) : (a) the filled-state image for (4×1) , (b) the empty-state image for (4×1) , (c) the filled-state image for (4×2) , and (d) the empty-state image for (4×2) . The filled- (empty-) state image is obtained by integrating the charge from Fermi level E_F to $E_F + 1.0$ (-1.0) eV. The images were obtained at 3.1 Å above the Si surface chain.

TABLE I. Calculated atomic displacements of In and Si atoms in the (4×2) structure, relative to their positions in the (4×1) structure. Si_{sub1} (Si_{sub2}) represents the Si atoms in the subsurface, bonding to the In (top-layer Si) atoms. The axes and labeling of atoms are shown in Fig. 1. The displacements are given in Å.

	Δx	Δy	Δz
$\text{In}_1(\text{In}_5)$	+0.137 (−0.143)	+0.046 (−0.048)	+0.004 (−0.001)
$\text{In}_2(\text{In}_6)$	+0.139 (−0.133)	+0.042 (−0.050)	+0.001 (+0.009)
$\text{In}_3(\text{In}_7)$	+0.126 (−0.064)	+0.122 (−0.107)	+0.024 (+0.035)
$\text{In}_4(\text{In}_8)$	+0.063 (−0.125)	+0.102 (−0.130)	+0.032 (+0.013)
$\text{Si}_1(\text{Si}_3)$	+0.019 (−0.022)	+0.029 (−0.032)	−0.002 (−0.008)
$\text{Si}_2(\text{Si}_4)$	+0.021 (−0.020)	+0.031 (−0.030)	−0.010 (−0.005)
Si_{sub1}	$\sim \pm 0.008$	$\sim \pm 0.003$	$\sim +0.025$
Si_{sub2}	$\sim \pm 0.003$	$\sim \pm 0.005$	$\sim \pm 0.005$

as well as the (8×2) structure do not support the CDW formation, where a total energy gain occurs from the electronic contribution due to a band gap opening at the Fermi level. Instead, the small energy gain in the (4×2) and (8×2) structures can be attributed to the energy lowering through the charge redistribution between the indium atoms, accompanied by lattice distortions (as discussed below). Note that in the (4×2) structure the lattice distortions lead to band splittings of 170 and 18 meV, respectively, for the unoccupied S_2 and occupied S_3 states at the X point [see Fig. 2(b)]. Note that neither splitting results in states being pushed across the Fermi energy along the $X'M'$ line. The significant band splitting of S_2 shows that the lattice distortions largely affect the S_2 state which contains indium- p character. On the other hand, the lattice distortions yield a slight band splitting for the S_3 state which originates from Si substrate states.

We note that our surface-state energy bands for the (4×1) structure are in near perfect agreement with the photoemission data of Ref. 8, whereas our bands for the (4×2) structure are inconsistent with the 1D-CDW interpretation of the photoemission data in Ref. 2 because no important energy gaps are opened up at the Fermi surface. While it is possible that this is a consequence of our bulk energy gap being only about 60% of its experimental value (consistent with every other local-density-approximation and GGA calculation, and having no effect on ground-state properties), we think it more likely that the authors of Ref. 2 misinterpreted their data. They compared the photoemission from a (4×2) structure with that from a (4×1) structure for several values of \mathbf{k} along the ΓX line. They found a reduction in spectral weight within 1 eV of the Fermi energy for most \mathbf{k} and within 2 eV for some \mathbf{k} . For only two values of \mathbf{k} is any increase in the spectral weight observed, and that is more than 1 eV below E_F . This is perfectly consistent with our band structures. We note that all surface states around the X point in the (4×1) SBZ are folded back around the Γ point in the (4×2) SBZ, where they become continuum states. To the extent that these states become bulklike (as opposed to narrow surface resonances), they will only contribute to the photoemission when there exists a wave-vector and energy-conserving final state. Thus the reduction in spectral weight is accounted for.

There are three possible (8×2) structures for a given left-hand chain in Fig. 1(d). Note that atom 1 (5) is displaced along the positive (negative) x direction in both chains, while the displacements of atoms 2 and 6 are negative and positive in the left-hand chain and positive and negative in the right-hand chain. The other two possibilities are 1 and 5 reversed or both 1 and 5 and 2 and 6 reversed in the right-hand chain. The reversal of a single pair results in the glide planes seen in the x-ray data,³ and is shown in Fig. 1(d). Our choice of which pair to reverse was arbitrary, but, since the energy difference between the two (8×2) choices is expected to be much smaller than the tenths of a meV difference between the (4×2) and (8×2) structures, it is pointless to calculate it. Because of this very small energy difference between the (8×2) structures, one would expect very little correlation between the (4×2) subcells along the chains. This explains the recent experimental observation³ that half-order streaks along the indium chains remain in the x-ray-diffraction pattern even 20 K.

The relative atomic positions in the (4×2) subcell of the (8×2) structure are very close to those in the (4×2) structure. The atomic displacements in the (4×2) structure relative to the (4×1) structure are given in Table I. The outer indium atoms in the (4×2) and (8×2) structures are displaced alternatively to form pairs [see Figs. 1(c) and 1(d)]. The distance of the paired indium atoms is reduced to 3.59 Å, compared with the corresponding distance of 3.87 Å in the (4×1) structure. Such pairings relax the inner indium atoms 3 and 8 (4 and 7) toward (away from) the center of the indium chain. Here our optimized structure shows that the indium atom 3 (8) is closer to the indium atom 4 (7), indicating some attraction between those atoms. The distances $d_{\text{In}_3-\text{In}_4}$ and $d_{\text{In}_7-\text{In}_8}$ become shorter, 3.06 Å, compared to 3.12 Å in the (4×1) structure. This rearrangement of indium atoms in the (4×2) structure changes the simulated STM images. We find that in the filled- and empty-state images the interstitial regions between the indium pairs appear dark or of reduced brightness [see Figs. 3(c) and 3(d)]. The filled-state image for the (4×2) structure shows a large difference compared with the STM result of Ref. 2 in that bright protrusions were observed with $2a_{[1\bar{1}0]}$ periodicity along the indium chains. However, the (4×1) filled-state

image of Ref. 2 also disagrees with Fig. 3(a) as well as the experimental images of Refs. 5 and 6 [which did not have (4×2) images] in that the latter have double-row images whereas Ref. 2 has its brightest region in the center of the double row.

A recent x-ray-diffraction experiment³ reported that at low temperature the periodicity along the indium chains doubles due to a pairing effect of the outer indium atoms, resulting in the formation of indium trimers where the interatomic distances are between 2.8 and 3.1 Å. However, in our (4×2) structure the corresponding distances within the trimers, composed of the indium atoms 1-3-5 (2-6-8), are $d_{\text{In}_1-\text{In}_3}=3.08$ Å, $d_{\text{In}_3-\text{In}_5}=3.00$ Å, and $d_{\text{In}_1-\text{In}_5}=3.59$ Å ($d_{\text{In}_2-\text{In}_8}=3.01$ Å, $d_{\text{In}_6-\text{In}_8}=3.09$ Å, and $d_{\text{In}_2-\text{In}_6}=3.60$ Å). Here the separation between the outer indium atoms (1-5 and 2-6) is larger than the x-ray-diffraction result.³ We believe our calculations are sufficiently accurate to distinguish energy differences between different structures of 1 meV per (4×1) unit cell, but we are unable to say why the interpretation of the (4×2) structure x-ray data disagrees with our calculated atomic positions. We note that our energy differences of 8 and 0.9 meV correspond to temperatures of 92.8 and 10.4 K, consistent with the transition temperatures of 100 and 20 K. Our picture of the phase transitions is as follows. The (4×2) structure [Fig. 1(c)] is the basic unit. Note that we have chosen a unit cell where atoms In 1 and In 5 move toward each other and atom In 2 moves down toward atom In 6 on the lower edge of the cell. Because atoms In 2 and In 6 are on reflection planes of the (4×1) structure, a degenerate state would be obtained if we had chosen atom In 2 to move up and atom In 6 to move down. Note from Table I that atoms In 1 and In 5 do not move equally toward each other, their equivalence being destroyed by the motion of atoms In 2 and In 6. Thus this degenerate state also requires changes in the positions of all the other atoms in the unit cell. Similarly atoms In 1 and In 5 could move apart, bonding with neighbors outside the chosen unit cell. Thus each (4×2) unit cell has four degenerate configurations. Above 100 K the atoms oscillate between their energy minima, their average positions yielding a (4×1) structure. Between 100 and 20 K the atoms in each (4×2) cell are frozen randomly into one of the four degenerate ground states. The (8×2) structure consists of two (4×2) structures which are very weakly coupled through the Si chain. Note that opposite In 2-6 pairs [e.g., those on the two glide planes shown in Fig. 1(d)] are displaced in opposite directions. This splits the two-fold degeneracy of every one-electron state that would occur if the two (4×2) structures were identical and therefore lowers the total energy. An almost identical result would be expected if we had opposing In 2-6 pairs move together and opposing In 1-5 pairs move oppositely.¹² One might think that if both In 1-5 and In 2-6 opposing pairs move oppositely, the difference between the (8×2) and (4×2) binding energies would be twice that calculated by us, yielding a transition temperature of 20.8 K. However, that would destroy the glide planes observed in the x-ray data.

X-ray photoemission spectroscopy (XPS) provides useful information about the charge redistribution around surface

atoms by measuring core-level binding energies. Our initial-state theory calculations¹³ for the (4×1) structure predict that the almost degenerate $4d$ core levels of the inner indium atoms 3 and 4 are shifted to lower binding energy by 0.46 eV, relative to those of the outer indium atoms 1 and 2. This initial-state result is in excellent agreement with XPS experiment,⁹ in which two well-resolved core-level peaks are separated by 0.47 eV. While final-state effects can be important, their calculation involves removing a core electron from an atom in a supercell, and restoring charge neutrality by adding one more conduction-band electron per supercell. The error introduced by the addition of these extra electrons is uncertain, but it is certainly enhanced when the only conduction-band states are localized on the surface. Past experience shows that final-state contributions sometimes improve agreement with experiment and sometimes worsen it. For example, we have found¹⁴ that the $4f$ initial-state surface core-level shift (SCLS) at the W(110) surface is -0.25 eV (relative to the bulk), whereas the final-state SCLS is -0.30 eV and the experimental value is -0.31 eV. On the other hand, the initial, final, and experimental values for the step edge atom on W(320) are -0.34 , -0.23 , and -0.41 eV, respectively. Thus our initial-state calculations here are as least as likely to be accurate as final-state calculations, but their near-perfect agreement with experiment could be fortuitous and should only be taken as an additional indication of the accuracy of our (4×1) structure. Our results for the (4×2) and (8×2) structures (for which there are no experimental results) show that the $4d$ core levels of both the inner and outer indium atoms are split into two additional components: The core levels of the indium atoms 1 and 6 (4 and 7) are shifted to lower binding energy by 0.05 (0.08) eV, relative to those of atoms 2 and 5 (3 and 8). These splittings in the indium- $4d$ core levels clearly indicate the charge redistribution around the indium atoms after the lattice distortions.

In summary, the atomic and electronic structures of quasi-1D indium chains on the Si(111) surface have been investigated by first-principles density-functional theory calculations. Excellent agreement with experiment was found for the (4×1) structure. We found that the (4×2) and (8×2) reconstructions consist mainly of a pairing of the outer indium atoms in the chain, qualitatively in agreement with a recent x-ray-diffraction measurement. However, our results for the lattice distortions and the band structure are not compatible with a simple quasi-1D CDW formation. We also argued that a (4×1) structure results above 100 K as a consequence of it representing the average positions of atoms vibrating between equivalent minima in the (4×2) structure, and that the (8×2) structure occurs only at very low temperatures because of the extremely weak coupling between the In chains in neighboring (4×2) structures which are separated by Si chains.

This work was supported by the National Science Foundation under Grant No. DMR-0073546 and the Welch Foundation (Houston, TX). K.S.K. acknowledges the support from Creative Research Initiatives of the Korean Ministry of Science and Technology.

- ¹P. Segovia, D. Purdie, M. Hengsberger, and Y. Baer, *Nature* (London) **402**, 504 (1999).
- ²H.W. Yeom, S. Takeda, E. Rotenberg, I. Matsuda, K. Horikoshi, J. Schaefer, C.M. Lee, S.D. Kevan, T. Ohta, T. Nagao, and S. Hasegawa, *Phys. Rev. Lett.* **82**, 4898 (1999).
- ³C. Kumpf, O. Bunk, J.H. Zeysing, Y. Su, M. Nielsen, R.L. Johnson, R. Feidenhans'l, and K. Bechgaard, *Phys. Rev. Lett.* **85**, 4916 (2000).
- ⁴J.L. Stevens, M.S. Worthington, and I.S.T. Tsong, *Phys. Rev. B* **47**, 1453 (1993).
- ⁵J. Kraft, M.G. Ramsey, and F.P. Netzer, *Phys. Rev. B* **55**, 5384 (1997).
- ⁶A.A. Saranin, A.V. Zotov, K.V. Ignatovich, V.G. Lifshits, T. Numata, O. Kubo, H. Tani, M. Katayama, and K. Oura, *Phys. Rev. B* **56**, 1017 (1997).
- ⁷O. Bunk, G. Falkenberg, J.H. Zeysing, L. Lottermoser, R.L. Johnson, M. Nielsen, F. Berg-Rasmussen, J. Baker, and R. Feidenhans'l, *Phys. Rev. B* **59**, 12 228 (1999).
- ⁸T. Abukawa, M. Sasaki, F. Hisamatsu, T. Goto, T. Kinoshita, A. Kakizaki, and S. Kono, *Surf. Sci.* **325**, 33 (1995).
- ⁹T. Abukawa, M. Sasaki, F. Hisamatsu, M. Nakamura, T. Kinoshita, A. Kakizaki, T. Goto, and S. Kono, *J. Electron Spectrosc. Relat. Phenom.* **80**, 233 (1996).
- ¹⁰N. Troullier and J.L. Martins, *Phys. Rev. B* **43**, 1993 (1991).
- ¹¹J.P. Perdew, K. Burke, and M. Ernzerhof, *Phys. Rev. Lett.* **77**, 3865 (1996); **78**, 1396(E) (1997).
- ¹²This assumption is based on the fact that the energy of noninteracting (4×2) 's is independent of the various pairing choices and the effect of opposing left- and right-hand chain pairs pairing oppositely is to lower the symmetry and split the degeneracies.
- ¹³The initial-state core-level shift is defined by the difference of the eigenvalues of a given core level at different sites. Here this shift is calculated from the expectation value of the self-consistent potential on the In $4d$ atomic orbital localized at each site [see J.-H. Cho, Z.Y. Zhang, S.H. Lee, and M.H. Kang, *Phys. Rev. B* **57**, 1352 (1998); **59**, 12 200 (1999)].
- ¹⁴J.-H. Cho, D.-H. Oh, and L. Kleinman, *Phys. Rev. B* **64**, 115404 (2001).